Pulse Vaccination Strategy in the SIR Epidemic Model

BORIS SHULGIN*
Department of Physics, Saratov State University,
Astrakhanskaya 83, Saratov, 410026, Russia

LEWI STONE
The Porter Super Center for Ecological and Environmental Studies, Saratov
State University, Astrakhanskaya 83, Saratov, 410026, Russia

ZVIA AGUR
Department Cell Research and Immunology,
Tel-Aviv University, Ramat-Aviv, Tel-Aviv 69978, Israel

Theoretical results show that the measles 'pulse' vaccination strategy can be distinguished from the conventional strategies in leading to disease eradication at relatively low values of vaccination. Using the SIR epidemic model we showed that under a planned pulse vaccination regime the system converges to a stable solution with the number of infectious individuals equal to zero. We showed that pulse vaccination leads to epidemics eradication if certain conditions regarding the magnitude of vaccination proportion and on the period of the pulses are adhered to. Our theoretical results are confirmed by numerical simulations. The introduction of seasonal variation into the basic SIR model leads to periodic and chaotic dynamics of epidemics. We showed that under seasonal variation, in spite of the complex dynamics of the system, pulse vaccination still leads to epidemic eradication. We derived the conditions for epidemic eradication under various constraints and showed their dependence on the parameters of the epidemic. We compared effectiveness and cost of constant, pulse and mixed vaccination policies.

1. INTRODUCTION

Currently, the guidelines for measles immunization in many areas of the Western world recommend a first vaccination dose at 15 months of age and a second dose at around 6 years. These guidelines are based on the conventional concept of time-constant immunization strategies.

Recently, a new vaccination strategy against measles, pulse vaccination, has been proposed. This policy is based on the suggestion that measles epidemics can be more efficiently controlled when the natural temporal process of the epidemics is antagonized by another temporal process (Agur, 1985; Agur and Deneubourg, 1985; Agur et al., 1993). Theoretical results show that the 'pulse' vaccination strategy can be distinguished from the conventional strategies in leading to disease

---

eradication at relatively low values of vaccination (Agur *et al.*, 1993). In contrast, it is predicted that conventional vaccination strategies lead to epidemic eradication if the proportion of the successfully vaccinated individuals is higher than a certain critical value, which is approximately equal to 95% for measles (Anderson and May, 1995).

Pulse vaccination has gained in prominence as a result of its highly successful application in the control of poliomyelitis and measles throughout Central and South America (de Quadros *et al.*, 1991; Sabin, 1991). Another example for the application of this strategy is the United Kingdom, where, during November 1994, children aged 5 to 16 years were offered a single vaccination pulse, in the form of a combined measles and rubella (MR) vaccine. Coverage of 90% or more was achieved in 133 of 172 district health authorities (77%), and the mean coverage in England and Wales was 92%. As a result of this policy the number of cases of measles notified to the Office of Population Censuses and Surveys has fallen significantly. As a consequence it was concluded that pulse vaccination of all children of school age is likely to have a dramatic effect on the transmission of measles for several years and prevent a substantial toll of morbidity and mortality (Ramsay *et al.*, 1994).

However, some questions may arise concerning the expected impact of this strategy. On a practical level it seems essential to determine *a priori* the pulse interval required for the efficient implementation of the strategy. Simulations of the pulse model show that for Israel an interval of about 5 years between successive vaccination pulses prevents epidemics (Agur *et al.*, 1993). A simplified analysis of the model suggests that this interval is roughly similar to the average age of infection. Evaluation of this parameter in unvaccinated populations in developed countries as 5 years (Sabin, 1991) supports this analysis (Agur *et al.*, 1993).

Recently, the pulse vaccination strategy has been explored in simple steady-state and dynamic age-structured compartmental models (Nokes and Swinton, 1995). The problem of pulsed mass-action chemostat has been considered by Funasaki and Kot (1993) in a similar fashion.

The implementation of pulse strategy should depend on the ability to predict the resulting dynamics. In this context it is important to note that chaotic dynamics have been detected in measles epidemics in some European and American cities [notably (Olsen and Schaffer, 1990; Sugihara and May, 1990) etc.] and that mathematical models are able to predict the onset of chaotic epidemics (Schaeffer and Kot, 1985; Grenfell, 1992; Engbert and Drepper, 1994) as the result of seasonal variation in the contact rate (London and Yorke, 1973). Therefore, it seems important to examine what effect a mass pulse vaccination strategy will have on the periodic and chaotic epidemics dynamics which originate in seasonally forced measles models.

2. THE SIR MODEL

We study a population which is composed of three groups of individuals: susceptibles (S), infectious (I) and recovered (R), whose dynamics are modelled by the standard SIR equations with vital dynamics:

$$\frac{dS}{dt} = m - (\beta I + m)S$$

$$\frac{dI}{dt} = \beta I S - (m + g)I \qquad (1)$$

$$\frac{dR}{dt} = gI - mR.$$

The population has a constant size, which is normalized to unity:

$$S(t) + I(t) + R(t) = 1. \qquad (2)$$

For this model, S represents the proportion of individuals susceptible to the disease, who are born and die at the same rate m, and have mean life expectancy $1/m$. Susceptibles become infectious at a rate βI, where I is the proportion of infectious individuals and β is the contact rate. Infectious individuals recover (i.e., acquire long life immunity) at a rate g, so that $1/g$ is the mean infectious period. Infected individuals who have recovered are denoted by the proportion R. In practice, the equation for dR/dt is redundant because R can be obtained from the relation (2). A detailed description of the model and its dynamics may be found in Anderson and May (1995) and in Hethcote (1989). We note for future reference that in this article we use typical parameters that are representative of measles dynamics, as follows (Engbert and Drepper, 1994):

$$m = 0.02, \ \beta = 1800, \ g = 100. \qquad (3)$$

The dynamical system (1) has two equilibrium points. The first, corresponding to a population with no infected individuals, is referred to henceforth as the 'infection-free equilibrium':

$$S_0^* = 1 \qquad (4)$$

$$I_0^* = 0,$$

Here, as elsewhere below, the asterisk used in (4) indicates that the attached quantity is evaluated at equilibrium.

The second equilibrium corresponds to the case in which there is a significant group of infectious individuals, and which will be referred to as the 'epidemic

equilibrium':

$$S_1^* = \frac{m + g}{\beta} \tag{5}$$

$$I_1^* = \frac{m(R_0 - 1)}{\beta}, \tag{}$$

where the basic reproductive rate of the epidemic, R_0, is defined as in Anderson and May (1993):

$$R_0 = \frac{\beta}{m + g} = 1/S_1^*. \tag{6}$$

If $R_0 > 1$, then on average, each infected individual infects more than one other member of the population and a self-sustaining group of infectious individuals will propagate. A simple linear analysis shows that in this case, the 'epidemic equilibrium' point (S_1^*, I_1^*) is locally stable, while the 'infection-free' equilibrium point (S_0^*, I_0^*) is unstable. Conversely, if $R_0 < 1$ the epidemic cannot maintain itself because each infected individual on average, infects less than one member of the population. The 'epidemic equilibrium' (S_1^*, I_1^*) is then unstable (in fact, I_1^* becomes negative), while the 'infection-free' equilibrium point (S_0^*, I_0^*), is locally stable. It has been shown that for both the above cases, local stability of the equilibrium implies global stability in the meaningful domain for S and I (see Hethcote, 1989).

3. VACCINATION STRATEGIES

3.1. *Constant vaccination.* According to the conventional constant vaccination strategy, all new-born infants should be vaccinated, and p is the proportion of those vaccinated successfully (with $0 < p < 1$). In effect, constant vaccination reduces the birth rate, m, of susceptibles (Schenzle, 1984), so that the first equation of (1) becomes:

$$\frac{dS}{dt} = (1 - p)m - (\beta I + m)S. \tag{7}$$

An examination of the local stability of the equilibria of the SIR model with constant vaccination (7) reveals that there is a critical vaccination proportion p_c,

$$p_c = 1 - \frac{1}{R_0}. \tag{8}$$

which governs the dynamics of the system as follows:

(a) For relatively large vaccination levels, i.e., $p > p_c$, the 'infection-free' equilibrium point (4) is stable, with new coordinates $(I_0^{*'} = 0, S_0^{*'} = (1 - p))$.

(b) For relatively weak vaccination, i.e., $p < p_c$, the 'epidemic equilibrium' point (5) is stable and has the new coordinates

$$S_1^{*'} = S_1^*,$$

$$I_1^{*'} = I_1^* - \frac{m}{m + g} p.$$

Hence, increasing the vaccination proportion, p, linearly reduces the equilibrium number of infectious individuals, but the number of susceptibles remains unaffected.

It is useful to note that for the standard measles parameters (3),

$$p_c \simeq 0.95. \tag{9}$$

This means that for the constant vaccination scheme to be successful, i.e., for stabilization of the 'infection-free' equilibrium, it is necessary to immunize at least 95% of all children soon after birth. In practice, it is both difficult and expensive to implement vaccination for such a large population coverage. We are therefore led to examine the potential of other strategies such as pulse vaccination.

3.2. Pulse vaccination. Instead of constantly vaccinating an extremely large proportion of all newborn susceptibles, the pulse vaccination scheme proposes to vaccinate a fraction p of the entire susceptible population in a single pulse, applied every T years. Pulse vaccination gives life-long immunity to pS susceptibles who are, as a consequence, transferred to the 'recovered' class (R) of the population. Immediately following each vaccination pulse, the system (1) evolves from its new initial state without being further affected by the vaccination scheme until the next pulse is applied.

The theory of pulse vaccination has been outlined in Agur *et al.* (1993). The underlying principle is to apply vaccination pulses frequently enough so as to prevent the infectious population from ever growing, i.e., by maintaining $dI/dt < 0$ for all time. Such a strategy ensures that $I(t)$ is a decreasing function of time, and the infectious population will eventually dwindle to zero. It is easy to see from (1) that the condition $dI/dt < 0$ will always be fulfilled if S is permanently held below the *epidemic threshold*, S_c (Agur *et al.*, 1993):

$$S(t) < \frac{m + g}{\beta} = S_c. \tag{10}$$

The above discussion immediately suggests the strategy of applying pulse vaccination whenever $S(t)$ grows to a level that is close or equal to the threshold value

S_c. It has been shown (Agur *et al.*, 1993) that for this 'threshold method', periodic pulsing can maintain $S(t)$ below S_c as long as the period of pulsing T is kept below a fixed critical value T_{max}. Obviously, the longer the period between vaccination pulses, the less often it is necessary to vaccinate the susceptible population. But should the pulse interval exceed T_{max}, the vaccination scheme may fail. One of the main goals of this paper is to find a suitable technique for estimating this key parameter, T_{max}.

4. DYNAMICS OF SIR MODEL UNDER PULSE VACCINATION

When pulse vaccination is incorporated into the SIR model (1), the system becomes non-autonomous and may be rewritten as follows:

$$\frac{dS}{dt} = m - (\beta I + m)S - p \sum_{n=0}^{\infty} S(nT^-)\delta(t - nT)$$

$$\frac{dI}{dt} = \beta I S - (m + g)I.$$

$$(11)$$

where

$$S(nT^-) = \lim_{\epsilon \to 0} S(nT - \epsilon), \quad \epsilon > 0 \tag{12}$$

is the left-hand limit of $S(t)$, and $\delta(t)$ is the Dirac delta-function (Agur *et al.*, 1993). Pulse vaccination is applied as an impulse at the discrete times $t = nT$ ($n = 0, 1, 2, \ldots$), and the moment immediately before the n-th vaccination pulse is notated here as $t = nT^-$. The train of impulses generated by the delta-function in (11) creates jump discontinuities in the variable $S(t)$, which suddenly decreases by the proportion p whenever $t = nT$.

We begin the analysis of (11) by first demonstrating the existence of an 'infection-free' solution, in which infectious individuals are entirely absent from the population permanently i.e.,

$$I(t) = 0, \quad t \geq 0. \tag{13}$$

This is motivated by the fact that $I^* = 0$ is an equilibrium solution for the variable $I(t)$, as it leaves $dI/dt = 0$ [see (11)]. Under these conditions we show below that the susceptible population S oscillates with period T, in synchronization with the periodic pulse vaccination. In the section that follows we determine the stability conditions of this 'infection-free' solution.

Assuming (13), the growth of susceptibles in the time-interval $t_0 = (n - 1)T \leq t \leq nT$ must satisfy:

$$\frac{dS}{dt} = m(1 - S) - p\,S(nT^-)\delta(t - nT), \tag{14}$$

and has the solution:

$$S(t) = 1 + (S^\dagger - 1)e^{-m(t-t_0)} - p\,(1 + (S^\dagger - 1)e^{-mT}) \int_{t_0}^{t} \delta(t - nT). \quad (15)$$

Here, $S^\dagger = S(t_0)$ is the number of susceptibles S immediately after the $(n-1)$-th vaccination pulse at time $t_0 = (n-1)T$.

Using notation $Q(t) = 1 - (1 - S^\dagger)e^{-m(t-t_0)}$, we can rewrite the solution (15) as:

$$S(t) = \begin{cases} Q(t), & t_0 = (n-1)T \le t < nT \\ (1-p)Q(t), & t = nT. \end{cases} \quad (16)$$

Thus, (16) consists of two terms. The first one $Q(t)$ is the number of susceptibles between the two pulses occurring at $t = (n-1)T$ and $t = nT$, whereas $(1 - p)Q(nT)$ represents the number of susceptibles immediately after the vaccination pulse.

The initial condition $S^\dagger$ may change from one pulse interval to another in a manner that is straightforward to calculate. Setting $S^\dagger(n) = S(nT) = S_n$, it is possible to deduce the stroboscopic map F such that:

$$S_{n+1} = F(S_n). \quad (17)$$

The map F determines the number of susceptibles, $S(t)$, immediately *after* each pulse vaccination at the discrete times $t = nT$, and can be obtained from (16) and (17):

$$S_{n+1} = F(S_n) = (1-p)(1 + (S_n - 1)e^{-mT}). \quad (18)$$

The map F has the unique fixed point:

$$S^* = F(S^*) = \frac{(1-p)(e^{mT} - 1)}{p - 1 + e^{mT}}. \quad (19)$$

The fixed point S^* of the map F, implies that there is a corresponding cycle of period T in the susceptible population $S(t)$.

Under the assumption (13), the fixed point S^* is locally stable because:

$$\left| \frac{dF(S_n)}{dS} \right|_{S_n = S^*} = (1 - p)e^{-mT} < 1. \quad (20)$$

Thus, pulse vaccination yields the sequence S_n which must converge to the fixed point S^*.

Recall now that the map F determines the number of susceptibles $S(t)$, immediately *after* each pulse vaccination. As the orbit of the map converges to the fixed
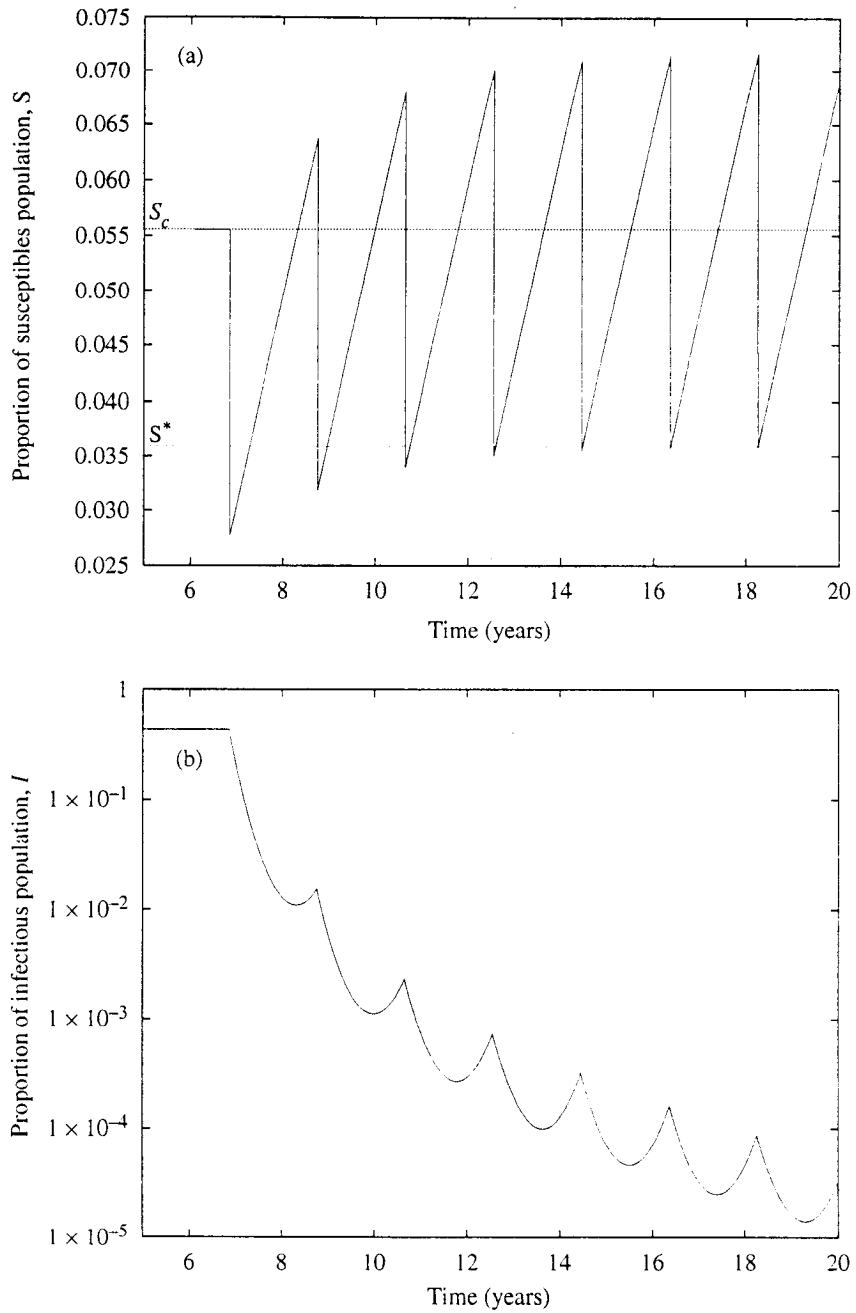
Figure 1. (a) Time-series of the susceptible population S evolving according to the pulse vaccination SIR model (11) with $p = 0.5$, $T = 2$. The sequence S_n [minima of $S(t)$], defined by the map (17), are indicated by the asterisks and converge to the fixed point $S^* \approx 0.036$ (19). The line at $S_c \approx 0.0556$ marks the 'epidemic threshold'. (b) Time-series for the corresponding infectious population I on a logarithmic scale.

point S^*, the evolution of the susceptible population $S(t)$ converges to the periodic cycle (15) [see Fig. 1.(a)]. Therefore, by setting $S^* = S^*$ in (15), we obtain the complete expression for the 'infection-free' periodic solution over the n-th time-interval $t_0 = (n - 1)T \leq t \leq nT$:

$$\tilde{S}(t) = 1 - \frac{pe^{mT}}{e^{mT} - (1 - p)}e^{-m(t-t_0)}$$

$$-p\left(1 - \frac{pe^{mT}}{e^{mT} - (1 - p)}e^{-mT}\right)\int_{t_0}^{t}\delta(t - nT) \qquad (21)$$

$$\tilde{I}(t) = 0.$$

The solution is periodic in time: $\tilde{S}(t + T) = \tilde{S}(t)$, $\tilde{I}(t + T) = \tilde{I}(t)$.

4.1. Stability of the periodic 'infection-free' solution. The stability of the 'infection-free' solution is found by linearizing the SIR equations (11) about the known periodic solution (21) by setting:

$$S(t) = \tilde{S}(t) + s$$

$$\qquad (22)$$

$$I(t) = \tilde{I}(t) + i$$

where s and i are small perturbations. Equation (11) can then be expanded in a Taylor series and, after neglecting higher order terms, the linearized equations read:

$$\frac{ds}{dt} = -ms - \beta\tilde{S}(t)i - ps(nT^-)\sum_{n=0}^{\infty}\delta(t - nT)$$

$$\qquad (23)$$

$$\frac{di}{dt} = i\,(\beta\tilde{S}(t) - m - g).$$

Note that the function $\tilde{S}(t)$ is known explicitly and should be viewed as a periodic coefficient of the variables s and i, respectively. The periodic solution of the full model (11) will be locally stable if the equilibrium $(i^*, s^*) = (0, 0)$ of the above linearized model is locally stable (Looss and Joseph, 1980).

Floquet theory provides a well-defined framework for examining stability of linear systems with periodic coefficients (Looss and Joseph, 1980). The first step requires constructing the fundamental matrix $A(t)$ of the linear system defined over the time interval $0 \leq t \leq T$ (Zwillinger, 1989):

$$[A(t)] = \begin{bmatrix} s_1(t) & s_2(t) \\ i_1(t) & i_2(t) \end{bmatrix}, \qquad (24)$$

where $(s_1(t), i_1(t))$ and $(s_2(t), i_2(t))$ are solutions, still yet to be derived, of the linear system (23) with the following initial conditions:

$$s_1(0) = 1 \quad s_2(0) = 0$$
$$i_1(0) = 0 \quad i_2(0) = 1. \tag{25}$$

Solving, we obtain:

$$i_1(t) = 0$$

$$s_1(t) = e^{-mt} - pe^{-mt} \int_0^t \delta(t - nT)\, dt$$

$$i_2(t) = e^{\int_0^t (\beta \tilde{S}(t) - (m+g))\, dt},$$

There is no need to calculate the exact form of $s_2(t)$ as it is not required in the analysis that follows.

The 'Floquet multipliers' are defined as the eigenvalues μ of the 'monodromy matrix' $A(T)$, i.e., they are solutions of the eigenvalue problem (Zwillinger, 1989):

$$Det([A(T)] - \mu[I]) = 0, \tag{26}$$

or,

$$Det \begin{bmatrix} (1-p)e^{-mT} - \mu & s_2(T) \\ 0 & i_2(T) - \mu \end{bmatrix} = 0. \tag{27}$$

The two Floquet multipliers are thus:

$$\mu_1 = (1-p)\, e^{-mT} < 1$$

$$\mu_2 = i_2(T) = e^{[\int_0^T \beta \tilde{S}(t) dt - (m+g)T]}. \tag{28}$$

According to Floquet theory, the solution (21) is locally stable if the absolute value of all Floquet multipliers are less than unity. Stability thus depends on whether:

$$|\mu_2| < 1. \tag{29}$$

From (28) we see that the 'infection-free' solution to the SIR model under pulse vaccination (11) is locally stable if:

$$\frac{1}{T} \int_0^T \tilde{S}(t) dt < \frac{m+g}{\beta} = S_c. \tag{30}$$

Thus for stability, the mean value of $\tilde{S}(t)$ averaged over a single pulse period must be less than the threshold level S_c. [This stability condition (30) can also be derived by using the stroboscopic map for $I(t)$, see Appendix 1]. Our extensive numerical investigations of the system (11) suggest that local stability of the 'infection-free solution' implies global stability in the meaningful domain for the variables S and I.

A typical solution of the SIR equation under pulse vaccination is shown in Fig. 1(a), where we may observe how the variable $S(t)$ oscillates in a stable cycle that periodically rises above the threshold level S_c. The oscillation is stable because the mean value of $S(t)$ over the inter-pulse periods is less than the threshold level S_c. In contrast, the infected individuals $I(t)$ rapidly decrease to zero.

The stability condition (30) can be fully specified by substituting the exact expression for $\tilde{S}(t)$ (21), and integrating. In terms of the model's parameters, local stability of the cycle is ensured if:

$$\frac{(mT - p)(e^{mT} - 1) + mpT}{mT(p - 1 + e^{mT})} < \frac{m + g}{\beta}. \tag{31}$$

It is possible to obtain an expression for the maximum allowable period of the pulse, T_{max}, in which the stability criterion above is satisfied. The maximum value occurs when there is equality in (31). [This is a consequence of the fact that the left-hand side of (31) is an increasing function of T.] In order to calculate T_{max} one can simplify (31) by using Taylor expansions by reasonably assuming the period of pulses is much shorter that the mean life-time, $T \ll 1/m$, and that the mean life-time of an individual is much longer than the duration of disease ($m \ll g$). After neglecting higher order terms we finally obtain:

$$T_{max} \simeq \frac{gp}{\beta m} \frac{1}{(1 - p/2 - g/\beta)}. \tag{32}$$

We now examine the earlier pulse vaccination formulation mentioned in Section 2.2, where pulses are applied frequently enough to ensure $dI(t)/dt < 0$ for all t, so that the number of infectious individuals is a decreasing function of time. According to (1), it is possible to satisfy this condition if pulsing ensures that for all t, $S(t) < S_c = (m + g)/\beta$, i.e., pulse vaccination is applied every time $S(t)$ approaches the threshold S_c. This 'threshold method' is amenable to analysis by the techniques already discussed here. Assume that pulse vaccination is applied periodically (with $T < T_{max}$) so that the susceptible population oscillates in a stable limit cycle according to (21). All that remains is to determine the maximum inter-pulse interval for which $S(t)$ stays permanently subthreshold.

Recall that the minimum number of susceptibles occurs just after pulse vaccination and is given by S^*, while the maximum number of susceptibles occurs just before vaccination and is equal to $S^*/(1 - p)$. Hence, to ensure $S(t) < S_c$, we require:

$$S^*/(1 - p) < S_c. \tag{33}$$
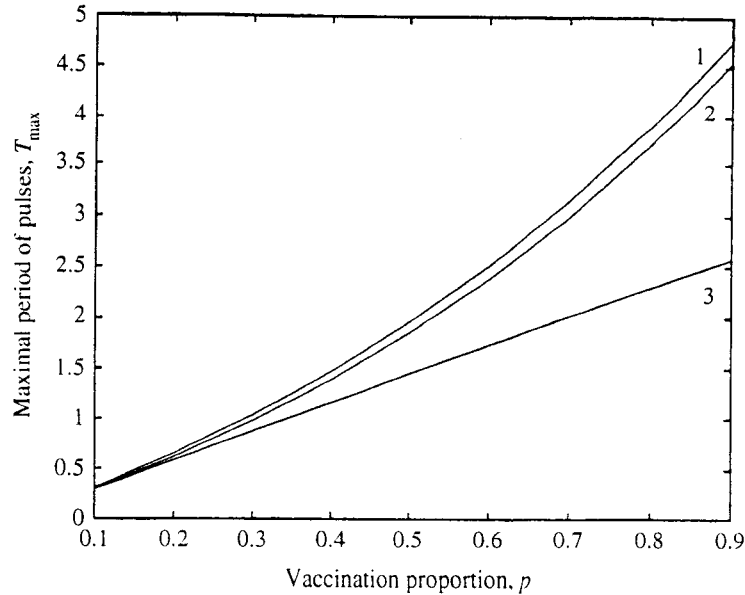
B. Shulgin et al.

Figure 2. The maximum inter-pulse interval T_{max} as a function of vaccination proportion, p. Curve 1: approximation (32). Curve 2: exact result (31). Curve 3: the result for the 'threshold condition' (34), (Agur *et al.*, 1993).

We can immediately arrive at an expression for T_{max} by evaluating (33) at equality and making use of (19):

$$T_{max} = \frac{1}{m} \ln \left(1 + \frac{pS_c}{1 - S_c} \right) \tag{34}$$

thus re-deriving the result in Agur *et al.* (1993).

Figure 2 compares the predictions for T_{max} derived from the new criterion (32) to the criterion of the earlier 'threshold method' (34) described in Agur *et al.* (1993) (i.e., which keeps $dI/dt < 0$). [The calculations are based on the standard measles parameters given above (3).] The figure also shows clearly that the simple expression approximating T_{max} via (32) is an excellent predictor of the exact results determined numerically by the criterion in (31). Also noteworthy is the fact that while constant vaccination is ineffective if the successful vaccinated proportion p is less than p_c (9), the pulse vaccination leads to an 'infection-free' population even at relatively small values of p if the period of pulse satisfies: $T < T_{max}$.

If period of pulses T is more than T_{max}, the 'infection-free solution' becomes unstable and variable I begins to oscillate with a large amplitude that corresponds to periodic bursts of epidemics. If the period of pulses is further increased a sequence of 'period addings' bifurcations interchanging with regions of chaos is observed (Fig. 3).
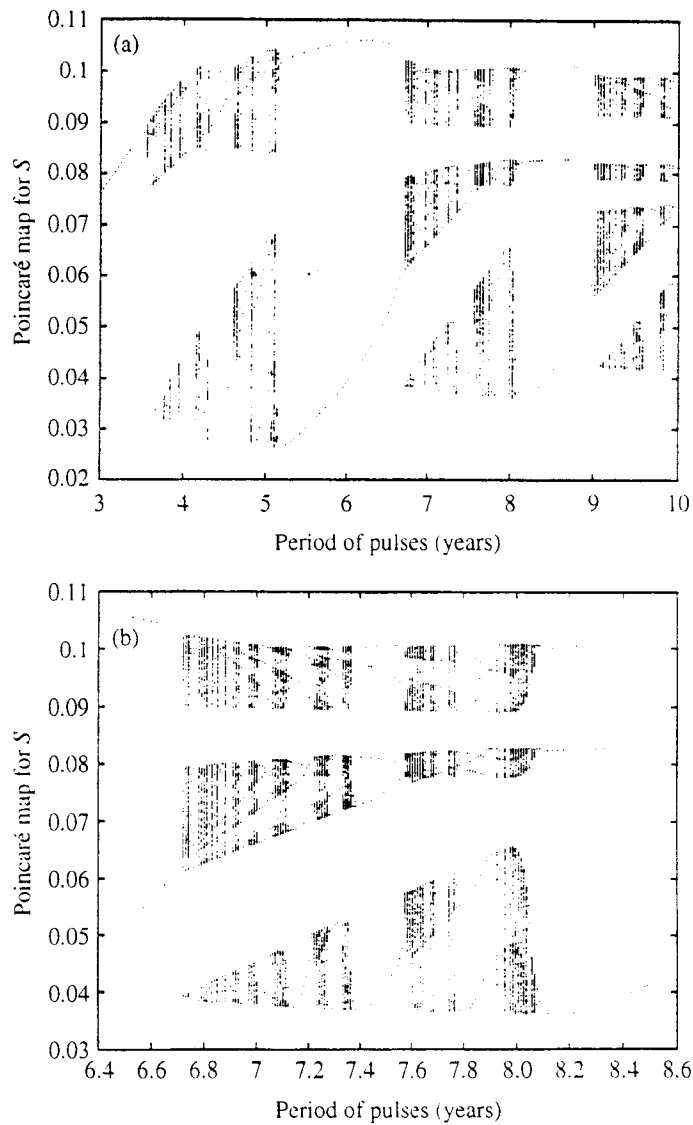
Figure 3. (a) Bifurcation diagram for the proportion of the susceptible population S under pulse vaccination ($p = 0.75$) as the inter-pulse interval T is varied. The points plotted correspond to the maxima of S when $dS(t)/dt = 0$ ($d^2S(t)/dt < 0$) thereby giving the Poincaré section. (b) A magnified part of the Fig. 3(a).

5. Effects of Pulse Vaccination on a Seasonally Forced SIR Model

The dynamics of the basic SIR model (1) are determined by the model's two equilibrium states (see Section 1). In the absence of external perturbation, all variables S, I and R eventually reach a constant equilibrium state. However, the epidemiological data on measles rarely suggest that an equilibrium state exists in practice. In contrast, measles data often demonstrate periodic or irregular outbreaks of the epidemic [e.g. Anderson and May (1982) and Dietz (1976)]; dynamics which the basic SIR model fails to capture. Moreover chaotic dynamics have been detected in measles epidemics in some European and American cities (Schaeffer and Kot, 1985; Grenfell, 1992; Engbert and Drepper, 1994). Yet the SIR model is 2-dimensional, and it is known that such systems never exhibit chaos.

More realistic dynamics may be achieved by taking into account the seasonal nature of the epidemic. London and Yorke (1973), for example, showed the importance of considering the contact rate β, as a periodic (annual) function of time. Sources of seasonal variation in the contact rate have been attributed to social behaviour, such as the timing of the school year, and seasonal changes in weather conditions (London and Yorke, 1973; Engbert and Drepper, 1994). Seasonal forcing in the SIR model is known to lead to more complex oscillatory and chaotic dynamical regimes simply because its inclusion makes the system 3-dimensional (the phase of periodic force can be written down as a new independent variable), providing it with the potential to generate more complex oscillatory solutions.

It is therefore important to examine how pulse vaccination will affect the complex dynamics realized in seasonally forced epidemiological models. After the introduction of seasonal variations in the contact rate, β, the SIR system (11) becomes:

$$\frac{dS}{dt} = m - (\beta(t)I + m)S - p \sum_{n=0}^{\infty} S(nT^-)\,\delta(t - nT)$$

$$\frac{dI}{dt} = \beta(t)IS - (m + g)I,$$

(35)

where

$$\beta(t) = \beta_0(1 + \beta_1 \cos 2\pi t), \quad \beta(t + 1) = \beta(t), \tag{36}$$

where β_0 is a constant value of the contact rate, and $0 \le \beta_1 \le 1$ determines the amplitude of seasonal variation (i.e., with a 1-year period).

In the absence of the vaccination ($p = 0$), the system (35) has a single 'infection-free' equilibrium point $(S_0^*, I_0^*) = (1, 0)$ which is stable if $R_0 = \beta_0/(m+g) < 1$ (see Appendix 2). However, for the measles parameters (3) $R_0 \gg 1$ and the 'infection-free' equilibrium is clearly unstable. The dynamics of the seasonally forced SIR model is then very much dependent on the amplitude of the seasonal variation

β_1 [see Schwartz (1985) and references therein, and also Aron (1990)]. Roughly summarized, as β_1 is increased from zero, the system changes from regular (limit-cycle) oscillations representing periodically recurrent epidemics, to deterministic chaos via a sequence of period doubling bifurcations. In the next section we show that these dynamics are altered dramatically in the presence of pulse vaccination (i.e., with $p > 0$).

5.1. Existence and stability of the 'infection-free' solution.

It is not difficult to see that the SIR equations (35) have the same 'infection-free' solution (21), both with and without seasonal forcing. This stems from the fact that the 'infection-free' solution has $I(t) = 0$ at all times, making the solution $S(t)$ completely independent of the seasonal forcing $\beta(t)$ [see (35)]. However, seasonal forcing does affect the stability of this periodic solution as we proceed to show.

In practice, the period of pulse vaccination, T, will be an integer valued number of years. In this case the right-hand side of (35) has period T, and Floquet techniques can be applied directly.

Linearizing the model (35) about the periodic solution, results in equations identical in form to (23) except that now the coefficient $\beta(t)$ is periodic in time. The Floquet multipliers of the system are thus:

$$\mu_1 = (1 - p)\, e^{-mT}, \quad |\mu_1| < 1$$

$$\mu_2 = i_2(T) = e^{\int_0^T \beta(t)\tilde{S}(t)dt - (m+g)T}. \tag{37}$$

Again, stability of the periodic 'infection-free' solution is ensured if the Floquet multiplier satisfies $|\mu_2| < 1$, i.e., if:

$$\frac{1}{T}\int_0^T \beta(t)\tilde{S}(t)dt < m + g. \tag{38}$$

As we know $\tilde{S}(t)$, it is possible to explore this stability criterion further. First, however, it is important to note that pulse vaccination may be applied at any time of year. This introduces a phase-shift φ_0 between oscillations of the susceptible population $\tilde{S}(t)$ and the seasonal variation of the contact rate $\beta(t)$. This phase-shift should be introduced into the seasonal force (36) as follows:

$$\beta(t) = \beta_0 + \beta_0\beta_1 \cos(2\pi t + \varphi_0).$$

Local stability of the 'infection-free' solution in seasonally forced model (35) is then ensured if:

$$\frac{1}{T}\int_0^T \beta(t)\tilde{S}(t)dt = \frac{\beta_0((1 - e^{mT})(p - mT) + mpT)}{mT(p - 1 + e^{mT})}$$

$$+ \frac{\beta_0\beta_1 p}{T}\left(\frac{(1 - e^{mT})(m\cos\varphi_0 - 2\pi\sin\varphi_0)}{(4\pi^2 + m^2)(p - 1 + e^{mT})}\right) < m + g. \tag{39}$$

It is possible to obtain an expression for the maximum allowable period of the pulse, T_{max}, in which the stability criterion above is satisfied. The maximum value occurs when there is equality in (39). [This is again a consequence of the fact that the left-hand side of (39) is an increasing function of T.] After applying Taylor expansions, assuming that $T \ll 1/m$, and that the mean lifetime of an individual is much greater than the duration of the disease, $m \ll g$, and using that $m \ll 2\pi$, we finally obtain:

$$T_{max} \simeq T_0 + T_1,$$

where

$$T_0 = \frac{pg}{\beta_0 m(1 - p/2 - g/\beta_0)}, \quad T_1 = \frac{p\beta_1(m \cos\varphi_0 - 2\pi \sin\varphi_0)}{4\pi^2(1 - p/2 - g/\beta_0)}. \tag{40}$$

Note that T_0 is the maximal period of pulsing obtained earlier for the case when there was no seasonal forcing (32). The term T_1, on the other hand, is directly dependent on seasonal forcing, via the parameter β_1. After substituting conventional measles parameters (3) the ratio T_1/T_0 is found to be:

$$\frac{T_1}{T_0} \leq \frac{\beta_1}{17} < 1/50. \tag{41}$$

Thus T_1 is less than 2% of T_0 and is, for all practical purposes, negligible. Hence the presence or absence of seasonal variations has little overall effect on T_{max}. However, for another range of parameters the influence of seasonal forcing could be more significant. In such cases, it may be necessary to check whether the phase shift φ_0 significantly influences T_{max}. If so, one could ascertain the optimal time of year to apply pulse vaccination. For example, for the given measles parameters, one finds that T_{max} has a maximum when:

$$\varphi_0 \cong 3\pi/2. \tag{42}$$

This suggests that in an optimal scheme, pulse vaccination should be applied approximately 3 months after the maximum in the seasonal contact rate $\beta(t)$ in order to achieve the longest possible inter-pulse interval T_{max}.

Assume now that the period of the product $\beta(t)S(t)$ in (35) can be considered to be irrational. In this case we average the condition of stability of 'infection-free' solution (38) by the equally distributed initial phase shift φ_0 in the interval $[0, 2\pi]$:

$$\left\langle \frac{1}{T} \int_0^T \beta(t; \varphi_0)S(t)dt \right\rangle_{\varphi_0} = \frac{1}{2\pi} \int_0^{2\pi} \frac{1}{T} \int_0^T \beta(t; \varphi_0)S(t)\, dt\, d\varphi_0 < m + g$$

or using (39):

$$\left\langle \frac{1}{T} \int_0^T \beta(t; \varphi_0)S(t)dt \right\rangle_{\varphi_0} = \frac{\beta_0 mT(1 - p/2)}{p + mT} < m + g. \tag{43}$$

Evaluating (43) at equality, we obtain the expression for T_{max},

$$T_{max} = \frac{pg}{\beta_0 m(1 - p/2 - g/\beta_0)} = T_0. \tag{44}$$

Once again our result show that the seasonal force does not affect the pulse vaccination scheme. But at the same time if there is no pulse vaccination ($p = 0$) the SIR system demonstrates periodic and chaotic behaviour as the result of seasonal forcing.

6. MIXED VACCINATION STRATEGY

Nokes and Swinton (1995) investigate an interesting strategy in which constant and pulse vaccination are applied simultaneously. Such a scheme is amenable to analysis by the methods we have described. With a mixed vaccination strategy the SIR dynamics are governed by:

$$\frac{dS}{dt} = m(1 - p_c) - (\beta I + m)S - p\sum_{n=0}^{\infty} S(nT^-)\delta(t - nT)$$

$$\frac{dI}{dt} = \beta I S - (m + g)I, \tag{45}$$

where p_c is the proportion of susceptibles who receive constant vaccination, and p is the proportion who receive pulse vaccination.

Once again there is a periodic 'infection-free' solution whose dynamics in the interval $(n - 1)T \geq t \leq nT$ $n = 0, 1, 2 \ldots$ are given by:

$$\tilde{S}(t) = (1 - p_c) + (S^+ - (1 - p_c))e^{-m(t-t_0)}$$

$$-p((1 - p_c) + (S^+ - (1 - p_c))e^{-mT})\int_{t_0}^{t} \delta(t - nT),$$

$$\tilde{I}(t) = 0, \tag{46}$$

where now,

$$S^+ = (1 - p_c)S^* \tag{47}$$

and S^* is given in (19).

The criterion for stability of the periodic 'infection-free' solution (46) may be found by the methods from Section 3.1 having as the result:

$$\frac{(1 - p_c)[(1 - e^{mT})(p - mT) + mpT]}{mT(p - 1 + e^{mT})} < \frac{m + g}{\beta}. \tag{48}$$
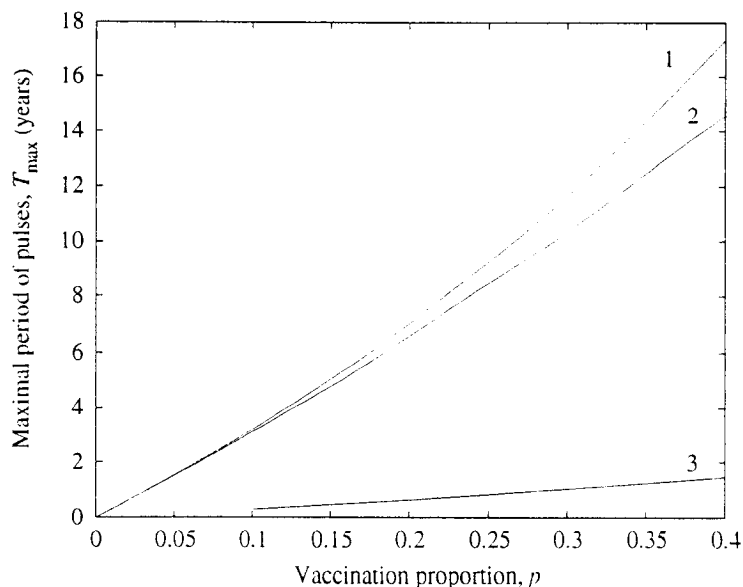
B. Shulgin et al.

Figure 4. The maximum inter-pulse interval T_{max} as a function of vaccination proportion, p. Curve 1. for the mixed vaccination strategy (constant vaccination proportion was set at $p_c = 0.85$). Curve 2. pulse vaccination only. Curve 3: with mixed vaccination scheme, which is safer, we can reach more longer periods of pulses.

The maximum pulse interval T_{max} for which the periodic solution is locally stable may be found by simplifying (48) at equality (as in Sections 3.1 and 4.1). After assuming that $T < (1 - p_c)1/m$ we obtain:

$$T_{max} \simeq \frac{gp}{\beta m} \frac{1}{[(1 - p_c)(1 - p/2) - g/\beta]} \simeq \frac{T_0}{1 - p_c},$$ (49)

where T_0 is maximal period of pulses for pulse vaccination only (32).

In other words the maximum inter-pulse interval T_{max} for the pulse vaccination scheme is a factor $(1 - p_c)$ shorter than the mixed scheme with constant vaccination proportion p_c. This big advantage of the mixed scheme is seen in the numerical simulations in Fig. 4, where we have plotted T_{max} as a function of the pulse vaccination proportion p, having set $p_c = 0.85$. The results show lie only in the realistic range $T_{max} < 20$ where the approximation (49) is reasonable. For comparison we have also plotted T_{max} as a function of p, for the pulse vaccination scheme only, i.e., without constant vaccination ($p_c = 0$).

7. ADDING REALISM TO THE SIR MODEL

One of the shortcomings of the SIR models is that the infective population may drop to unrealistically low levels of $I = 10^{-20}$ or less, while the value of I, corresponding to a single individual in a typical city of one million people, is $I = 10^{-6}$

(Engbert and Drepper, 1994; Anderson and May, 1982). In this case the SIR model simulates infectious populations of less than one individual. This feature is problematical when studying extinction dynamics where it is important to preserve the integer structure of the population.

Different schemes have been devised to solve the problem of unrealistic population levels. One approach is to make use of a stochastic version of the SIR model (Engbert and Drepper, 1994). Alternatively, for deterministic SIR-like models it is possible to prevent the population from dropping below the level of a single individual by buffering it with immigration and/or interaction that arises from contact with surrounding populations. The latter interaction is usually introduced via the 'force of infection' (Engbert and Drepper, 1994) term βI [see (1)] which should be modified to:

$$\beta(I + wI_1^*). \tag{50}$$

The term I_1^* is given by (5), and should be viewed as a surrogate for the size of the spatially averaged surrounding populations, while w represents the 'coupling constant' that links the populations.

The coupling changes the dynamics of the model considerably. For example, consider the second equation of the model (11):

$$\frac{dI}{dt} = I(\beta S - (m + g)) + \beta w I_1^* S. \tag{51}$$

The solution $I = 0$ is no longer an equilibrium state (i.e., with $dI/dt = 0$) for the infected population as previously, because now $w > 0$. Numerical computations show that even for very small inter-pulse intervals T, the infected population now oscillates rather than decays to zero (as would happen when $w = 0$ and there is an 'infection-free' solution). As there is no 'infection-free' solution we are led to define an epidemic outbreak when the infectious population I reaches a magnitude that is greater than some predefined threshold level I_c. For the purposes of analytical calculations detailed elsewhere (Shulgin, unpublished) we defined this threshold level to be:

$$I_c = \frac{m}{\beta} \simeq \frac{I_1^*}{(R_0 - 1)}. \tag{52}$$

Simulations reveal that increasing the inter-pulse interval T, increases the amplitude of the oscillations of the infectious population $I(t)$. In the simulations we gradually increased T until the peak of the oscillation attained the threshold level I_c. The value of T at which this occurred was defined as the maximum inter-pulse interval T_{max}.

The dependence of T_{max} on the vaccination proportion p is displayed in Fig. 5 for the modified model (51). Comparing these results with the unrealistic case, $w = 0$, one notes that when the infected population drops to unrealistic levels, the predicted values of T_{max} (30) can be up to 100% larger (for $p > 0.5$) than those obtained for $w > 0$.
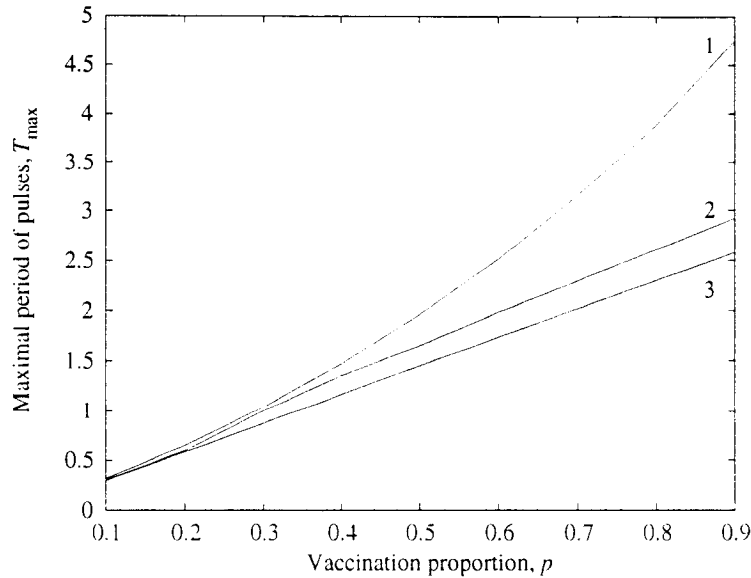
Figure 5. The maximum inter-pulse interval T_{max} as a function of vaccination proportion, p: Curve 1: condition (31) for the SIR model. Curve 2: for the modified model (51). Curve 3: condition $S(t) < S_c$ (34).

8. COST EFFECTIVENESS OF THE TWO VACCINATION SCHEMES

Recall that the constant vaccination scheme leads to a stable 'infection-free' equilibrium only if the vaccination proportion is greater than a critical value, which is approximately $p = 0.95$ for measles. In contrast, under pulse vaccination scheme the 'infection-free' equilibrium can be stable for arbitrarily small values of the vaccination proportion p, as long as an appropriate inter-pulse interval T is maintained. However, one needs to keep in mind that the number of people requiring immunization every T years under pulse vaccination, might be comparable with the number of infants requiring vaccination over the same T years, in the constant vaccination scheme. In the following section we attempt to compare the 'cost' (in terms of the mean number of individuals per year requiring vaccination) of the two strategies.

In the case of the constant vaccination the number of individuals vaccinated per year, $N(p)$, can be derived from (7):

$$N(p) = pm, \tag{53}$$

where, as before, the total population size has been normalized to unity (2). For the pulse vaccination scheme, the average number of people requiring vaccination per year is $N(p, T)$, which may be calculated as:

$$N(p, T) = \frac{1}{T} p S(nT^-), \tag{54}$$

where $pS(nT^-)$ is the number of people vaccinated by a pulse of vaccination applied at $t = nT$, $n = 0, 1, 2 \ldots$. Because $S(nT^-) = Q(nT)$ (15) and $S^\dagger = S^*$ [discussion before (21)], then:

$$S(nT^-) = \frac{e^{mT} - 1}{p - 1 + e^{mT}} \simeq \frac{mT}{p + mT}.$$

Thus,

$$N(p, T) \simeq \frac{pm}{p + mT}. \tag{55}$$

One can see that for a given value of p, (55) is minimized by choosing $T = T_{max}$ (32) and may be evaluated for measles as:

$$N(p, T_{max}) \simeq m - \frac{mg}{\beta(1 - p/2)} \simeq m. \tag{56}$$

We have obtained the minimum number of individuals requiring vaccination while simultaneously ensuring an 'infection-free' solution. This minimum number is approximated by m, and is largely independent of p. The interesting conclusion is that no matter what value of p or T_{max} is chosen, the minimum number of individuals to be vaccinated in this scheme is always the same. For an optimal pulse vaccination schedule, it makes little difference if pulses are applied every year ($T_{max} = 1$) or every 10 years ($T_{max} = 10$); almost the same number of people will be vaccinated.

Plotting (Fig. 6) the number of individuals requiring vaccination $N(p, T)$ as a function of p, showed that in this range constant vaccination scheme is superior to pulse vaccination, for $p < p_c \simeq 0.95$. Note, however, that constant vaccination is ineffective when $p < p_c = 0.95$, because it does not lead to eradication of the infection. For $p > p_c$, the 'cost', $N(p, T)$, of the two vaccination schemes is practically the same.

The main advantage of pulse vaccination is that it maintains a stable 'infection-free' solution for far smaller levels of the vaccination proportion, p. In practice, it is a much simpler task to target an intermediate proportion, say 70%, of the susceptible population in a campaign every few years (pulse vaccination) than to constantly ensure that a tight 95% coverage is achieved through every year (constant vaccination).

9. DISCUSSION

In this paper we analyse the pulse vaccination strategy (Agur *et al.*, 1993) in the SIR epidemic model [see also Stone *et al.* (in press)] We first examined the standard SIR model in which the system dynamics is characterized by two equilibria—an unstable 'infection-free' equilibrium and a stable 'epidemic equilibrium'. Earlier,
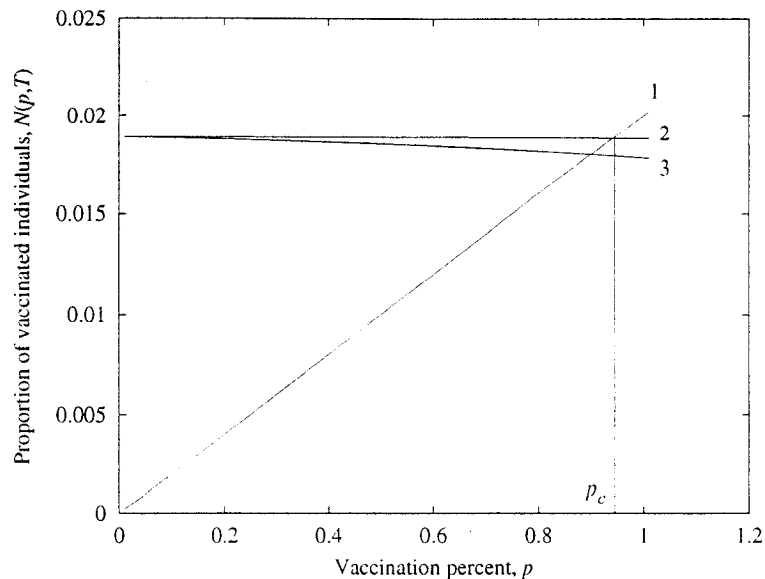
Figure 6. The proportion of people that are vaccinated *per annum* under constant and pulse schemes for various vaccination levels. Curve 1: constant vaccination, $N(p) = mp$. Curve 2: approximation $N(p, T) \simeq m$ for the pulse vaccination. Curve 3: equation (56) for the pulse vaccination.

Agur *et al.* (1993) showed that for the scheme to be successful in this model pulses should be applied frequently enough to keep $S(t)$ below the epidemic threshold S_c. In this case an epidemic outbreak can never occur by the definition of the epidemic threshold. Here we extended this study and showed that under pulse vaccination the system reaches a state of 'infection-free' even if $S(T)$ crosses the threshold for some time during the inter-pulse interval, but *the mean value of $S(t)$ during of inter-pulse interval* is kept under the threshold. This new condition allows us to use considerably longer periods of pulses (but recall the unrealistic aspects of the SIR model discussed above).

We have studied pulse vaccination in the seasonally forced SIR model, where periodic and chaotic epidemic outbreaks appear as a result of seasonal variations in the contact rate. We have shown that pulse vaccination suppresses these complex dynamics of the model and leads to the 'infection-free' solution, if the period of the pulses corresponds to the obtained criterion.

The advantage of the pulse vaccination strategy over the constant vaccination scheme is that in the former, low vaccination percentages suffice for preventing the epidemic outbreaks; in the case of constant vaccination $p > 0.95$ should be used. Note that pulse vaccination allows non-vaccination of part of the population. This can hardly be acceptable from a moral point of view. Another complication is that immigration of infection can cause epidemics when $S(t)$ crosses the threshold. For these reasons we suggest considering the mixed vaccination scheme as a possible alternative to the currently used strategy of a double dose constant vaccination. In the

mixed scheme the first (constant) vaccination, reduces the number of susceptibles by means of a high coverage vaccination percentage, and the second (pulse) vaccination of relatively low coverage with very long inter-pulse intervals, renders the 'infection-free' state a stable solution of the system. We have found the cost of the two schemes in units of people to be vaccinated to be approximately equal.

APPENDIX 1

The condition for stability of the 'infection-free' solution in pulse vaccinated SIR model (30) can also be studied with the stroboscopic map for $I(t)$ via the period of pulses T:

$$I_{n+1} = F(I_n),$$

where I_n is the number of infectious individuals at the moment of time following the n-th pulse.

From the second equation of the SIR model (11), we have:

$$I(t) = I(t_0)e^{\beta \int_{t_0}^{t} S(t)dt - (m+g)(t-t_0)}. \tag{57}$$

We can write a stroboscopic map for $I(t)$ via the period of pulses:

$$I_{n+1} = I_n e^{[\beta \int_{nT}^{(n+1)T} S(t)dt - (m+g)T]} = F(I_n). \tag{58}$$

The map (58) has a fixed point $I^* = F(I^*) = 0$, corresponding to an 'infection-free' population, which is stable if

$$\left| \frac{dF(I_n)}{dI} \right|_{I_n=I^*} = e^{\beta \int_{nT}^{(n+1)T} S(t)dt - (m+g)T} < 1. \tag{59}$$

From (59) we obtain

$$\frac{1}{T} \int_{nT}^{(n+1)T} S(t)dt < \frac{m+g}{\beta}, \tag{60}$$

which approaches (30) when $I(t)$ tends to zero.

Note that from (11) we can calculate the *per-capita* growth of infective and the stability condition (30) may then be rearranged as follows:

$$\left\langle \frac{dI/dt}{I} \right\rangle_T = \frac{1}{T} \left(\int_{nT}^{(n+1)T} \beta S(t) dt - (m+g)T \right) < 0. \tag{61}$$

This means that for the 'infection-free' solution to be locally stable, the *per-capita* growth of the infected population should, on average, be negative over the pulse period T.

APPENDIX 2

In the absence of vaccination ($p = 0$), the seasonally forced SIR model (35) has the unique equilibrium point ($S_0^* = 1, I_0^* = 0$). In this appendix we use Floquet theory to analyse the stability of the equilibrium.

Linearized about the equilibrium, the SIR equations (35) read:

$$\frac{ds}{dt} = -ms - \beta(t)i - p\, s(nT^-) \sum_{n=0}^{\infty} \delta(t - nT)$$

$$\frac{di}{dt} = i(\beta(t) - m - g), \tag{62}$$

where s and i are perturbations defined as in (22).

Following the procedures in Section 3.1, the Floquet multipliers of this system are found to be:

$$\mu_1 = (1 - p)e^{-mT} < 1,$$

$$\mu_2 = i_2(T) = e^{[\int_0^T (\beta(t)dt - (m+g)T]}. \tag{63}$$

Thus, the equilibrium is locally stable if

$$|\mu_2| < 1.$$

Rearranging (63) we see that the equilibrium point ($S = 1, I = 0$) is locally stable if

$$\frac{\beta_0}{m + g} = R_0 < 1.$$

REFERENCES

Agur, Z. (1985). Randomness synchrony and population persistence. *J. Theor. Biol.* **112**, 677–693.

Agur, Z. and J.L. Deneubourg. (1985). The effect of environmental disturbance on the dynamics of marine intertidal populations, *Theor. Pop. Biol.* **27**, 75–90.

Agur, Z., L. Cojocaru, G. Mazor, R. Anderson and Y. Danon (1993). Pulse mass measles vaccination across age cohorts. *Proc. Natl. Acad. Sci. USA* **90**, 11698–11702.

Anderson, R. and R. May (1982). Directly transmitted infectious diseases: control by vaccination. *Science*, **215**.

Anderson, R. and R. May (1995). *Infectious Diseases of Humans, Dynamics and Control* Oxford: Oxford University Press, pp. 1–757.

Aron, J.L. (1990). Multiple attractors in the response to a vaccination program. *Theor. Popul. Biol.* **38**, 58–67.

Dietz, K. (1976). In: *Mathematical Models in Medicine*, J. Berger, *et al.* (Eds), Lecture Notes in Biomathematics, Vol. 11, Springer-Verlag, pp. 1–15.

Engbert, R. and F. Drepper (1994). Chance and chaos in population biology—models of recurrent epidemics and food chain dynamics. *Chaos, Solutions & Fractals* **4**, 1147–1169.

Funasaki, E. and M. Kot (1993). Invasion and chaos in a periodically pulsed mass-action chemostat. *Theor. Popul. Biol.* **44**, 203–224.

Grenfell, B.T. (1992). Chance and chaos in measles dynamics. *J. Roy. Stat. Soc. B* **54**, 383–398.

Hethcote, M. (1989). Three basic epidemiological models, in *Applied Mathematical Ecology*, S. Levin *et al.* (Eds), Springer.

London, W. and J. Yorke (1973). Recurrent outbreaks of measles chickenpox and mumps. Part I. Seasonal variation in contact rates. *Am. J. Epidemiol.* **98**, 453–468.

Looss, G. and D.Joseph (1980). *Elementary Stability and Bifurcation Theory*, New York: Springer.

Nokes, D. and J. Swinton (1995). The control of childhood viral infections by pulse vaccination. *IMA J. Math. Appl. Biol. Med.* **12**, 29–53.

Olsen, L.F. and W.M. Schaffer (1990). Chaos versus noisy periodicity: alternative hypotheses for childhood epidemics. *Science* **249**, 499–504.

De Quadros, C.A., J.K. Andrus and J.M. Olivé (1991). Eradication of poliomyelitis: progress. *Am. Pediatr. Inf. Dis. J.* **10**, 222–229.

Ramsay, M., N. Gay and E. Miller (1994). The epidemiology of measles in England and Wales: rationale for 1994 national vaccination campaign. *Commun. Dis. Rep.* **4**, R141–R146.

Sabin, A.B. (1991). Measles, killer of millions in developing countries: strategies of elimination and continuing control. *Eur. J. Epidemiol.* **7**, 1–22.

Schaeffer, W.M. and M. Kot (1985). Nearly one dimensional dynamics in an epidemic. *J. Theor. Biol.* **112**, 403–427.

Schenzle, D. (1984). An age-structured model of pre- and post-vaccination measles transmission *IMA J. Math. Appl. Biol. Med.* **1**, 169–191.

Schwartz, I. (1985). Multiple stable recurrent outbreaks and predictability in seasonally forced nonlinear epidemic models. *J. Math. Biol.* **21**, 347–361.

Stone, L., B. Shulgin and Z. Agur (1998). Theoretical examination of the pulse vaccination policy in the SIR epidemic model, in *Proceedings of the Conference on Dynamical Sys-*

B. Shulgin et al.

tems in Biology and Medicine, Vesprem 1996, *Mathematical and Computer Modelling* in press.

Sugihara, G. and R.M. May (1990). Nonlinear forecasting as a way of distinguishing chaos from measurement error in time series. *Nature* **34**, 734–741.

Zwillinger, D. (1989). *Handbook of Differential Equations*, Academic Press.